Supplemental Material:
Accelerating K-Means Clustering for Document Data Sets with an Architecture-Friendly Pruning Method

Kazuo Aoyama
NTT Corporation
kazuo.aoyama@ntt.com

Kazumi Saito
Kanagawa University
k-saito@kanagawa-u.ac.jp

S1 FULL ALGORITHM OF AM-ICP

This section shows in Algorithms S1, S2, and S3 the pseudocode of the full algorithm of AM-ICP in Section 4.2. First, we show the pseudocodes of the assignment step, which correspond to Algorithms 2 and 3 and are rewritten in the form with scaling feature values [6]. The scaling is performed to avoid the multiplications for calculating the upper bounds on simialrities. Next, we detail the update step at the rth iteration in AF-ICP in Algorithm S3, which is not described in Section 4.2.

Algorithm S1 shows the assignment-step pseudocode. Scaling the data-object-feature values at lines 1 to 2 is performed once before our K-means clustering algorithm starts. Algorithm S2 shows G_1 function in Algorithm S1. Owing to scaling the data-object-feature values and mean-feature values at line 5 in Algorithm S3, we can obtain the upper bound on similarities by only the addition at line 9.

Algorithm S1   Assignment step in AF-ICP algorithm

Input: $\hat{X}$, $\check{\mathcal{M}}^{[r-1]}$, $\check{\mathcal{M}}^{p[r-1]}$, $\left\{\rho_{a(i)}^{[r-1]}\right\}_{i=1}^{N}$, $t^{[th]}$, $v^{[th]}$

Output: $C^{[r]} = \left\{C_j^{[r]}\right\}_{j=1}^{K}$

▷ Scale values before assignment step starts
1: **for all** $\hat{x}_i = [(t_{(i,p)}, u_{t_{(i,p)}})]_{p=1}^{(nt)_i} \in \hat{X}$ **do**
2:    $u_{t_{(i,p)}} \leftarrow \boxed{u_{t_{(i,p)}} \cdot v^{[th]}}$ ▷ Scaling

▷ Calculate similarities in parallel w.r.t $\hat{X}$
3: $C_j^{[r]} \leftarrow \emptyset$, $j = 1, 2, \cdots, K$
4: **for all** $\hat{x}_i = [(t_{(i,p)}, u_{t_{(i,p)}})]_{p=1}^{(nt)_i} \in \hat{X}$ **do**
5:    $\{\rho_j\}_{j=1}^{K} \leftarrow 0$, $\rho_{(max)} \leftarrow \rho_{a(i)}^{[r-1]}$, $\mathcal{Z}_i \leftarrow \emptyset$
6:    **for** $j \leftarrow 1$ **to** K **do**
7:        $y_{(i,j)} \leftarrow \sum_{t_{(i,p)} \geq t^{[th]}} (u_{t_{(i,p)}})$ ▷ Initializing $y_{(i,j)}$

▷ Gathering phase
8:    **if** $xState = 1$ **then**   ▷ ICP filtering
9:        $\left(\mathcal{Z}_i, \ \{\rho_j\}_{j=1}^{K}\right) = G_1(\mathcal{Z}_i, \{(\rho_j, \ y_{(i,j)}\}_{j=1}^{K}, \rho_{(max)}, (nMv))$
10:    **else**
11:        $\left(\mathcal{Z}_i, \ \{\rho_j\}_{j=1}^{K}\right) = G_0(\mathcal{Z}_i, \{(\rho_j, \ y_{(i,j)}\}_{j=1}^{K}, \rho_{(max)})$

▷ Verification phase
12:    **for** $(s \leftarrow t_{(i,p)}) \geq t^{[th]}$ **do**   ▷ Region 3
13:        **for all** $j \in \mathcal{Z}_i$ **do** $\rho_j \leftarrow \rho_j + u_s \cdot w_{(s,j)}$
14:    **for all** $j \in \mathcal{Z}_i$ **do**
15:        **If** $\rho_j > \rho_{(max)}$ **then** $\rho_{(max)} \leftarrow \rho_j$ and $a(i) \leftarrow j$
16:    $C_{a(i)}^{[r]} \leftarrow C_{a(i)}^{[r]} \cup \{\hat{x}_i\}$

Algorithm S2   Candidate-gathering function: G_1

Input: $\hat{x}_i$, $\check{\mathcal{M}}^{[r-1]}$, $t^{[th]}$, $v^{[th]}$, $\mathcal{Z}_i$, $\{\rho_j, y_{(i,j)}\}_{j=1}^{K}$, $\rho_{(max)}$,
   (nMv) ▷ (nMv): # moving centroids

Output: $\mathcal{Z}_i$, $\{\rho_j\}_{j=1}^{K}$
▷ Exact partial similarity calculation
1: **for** $(s \leftarrow t_{(i,p)}) < t^{[th]}$ in all term IDs in $\hat{x}_i$ **do**   ▷ Region 1
2:    **for** $\boxed{1 \leq q \leq (mfM)_s}$ **do**   ▷ Endpoint
3:        $\rho_{c_{(s,q)}} \leftarrow \rho_{c_{(s,q)}} + u_s \cdot v_{c_{(s,q)}}$
4: **for** $(s \leftarrow t_{(i,p)}) \geq t^{[th]}$ in all term IDs in $\hat{x}_i$ **do**   ▷ Region 2
5:    **for** $\boxed{1 \leq q \leq (mfM)_s}$ **do**   ▷ Endpoint
6:        $\rho_{c_{(s,q)}} \leftarrow \rho_{c_{(s,q)}} + u_s \cdot v_{c_{(s,q)}}$, $y_{(i,c_{(s,q)})} \leftarrow y_{(i,c_{(s,q)})} - u_s$

▷ Upper-bound calculation
7: **for** $\boxed{1 \leq j' \leq (nMv)}$ **do**
8:    $\boxed{j' \text{ is transformed to } j.}$
9:    $\rho_j^{[ub]} \leftarrow \rho_j + \boxed{y_{(i,j)}}$ ▷ Region 3 (UB): Scaling

▷ AF filtering
10:    **if** $\rho_j^{[ub]} > \rho_{(max)}$ **then** $\mathcal{Z}_i \leftarrow \mathcal{Z}_i \cup \{j\}$

Algorithm S3 shows the pseudocode of the update step at the rth iteration. The algorithm performs the following five processes at lines 1 to 16.

(1) Making tentative mean-feature vector λ of the cluster $C_j^{[r]}$ at lines 2 to 5. The λ with full expression consists of feature values λ_s ($s = 1, 2, \cdots, D$).

(2) Calculating the similarity $\rho_{a(i)}^{[r]}$ of the ith object to the centroid of cluster $C_{a(i)}^{[r]}$ to which the object belong at lines 6 and 7. $\rho_{a(i)}^{[r]}$ is utilized as the similarity threshold in the gathering phase at the assignment step at the next (r+1) iteration and for determining whether the ith object satisfies a condition with respect to the ICP filter in Section 4.2.

(3) Constructing mean-inverted index $\check{\mathcal{M}}^{[r]}$ and partial mean-inverted index $\check{\mathcal{M}}^{p[r]}$ using the obtained λ at lines 8 to 11. $\check{\mathcal{M}}^{p[r]}$ (its element $w_{(s,j)}$) is utilized for exact similarity calculations in Region 3 at the assignment step in Algorithm S1. $\check{\mathcal{M}}^{p[r]}$ consists of $(D - t^{[th]} + 1)$ inverted-index arrays $\check{\zeta}_s^{[r]}$ whose lengths are K. The jth element in $\check{\zeta}_s$ is mean-feature values $w_{(s,j)}$ if $w_{(s,j)} < v^{[th]}$, otherwise 0. Due to this full expression, the jth element can be directly accessed by using the centroid ID j as the key.

(4) Structuring inverted-index arrays for the AF filter, which are $\check{\zeta}_s^{[r]} \in \check{\mathcal{M}}^{[r]}$ ($t^{[th]} \leq s \leq D$) at lines 14 to 15. Since

Algorithm S3   Update step in AF-ICP algorithm

Input: $\hat{X}$, $C^{[r]} = \left\{ C_j^{[r]} \right\}_{j=1}^{K}$, $t^{[th]}$

Output: $\check{\mathcal{M}}^{[r]}$, $\check{\mathcal{M}}^{p[r]}$, $\left\{ \rho_{a(i)}^{[r]} \right\}_{i=1}^{N}$, $[(mfH)_s]_{s=t^{[th]}}^{D}$

1: **for all** $C_j^{[r]} \in C^{[r]}$ **do**
   ▷ (1) Making tentative mean-feature vector $\boldsymbol{\lambda}$
2:    $\boldsymbol{\lambda} = (\lambda_s)_{s=1}^{D} \leftarrow \mathbf{0}$ ▷ Tentative mean-feature vector
3:    **for all** $\hat{x}_i = \left[(t_{(i,p)}, u_{t_{(i,p)}}) \right]_{p=1}^{(nt)_i} \in C_j^{[r]}$ **do**
4:      $\lambda_{t_{(i,p)}} \leftarrow \lambda_{t_{(i,p)}} + u_{t_{(i,p)}}$
5:    $\boldsymbol{\lambda} \leftarrow \boldsymbol{\lambda}/|C_j^{[r]}|$, $\boldsymbol{\lambda} \leftarrow \boxed{\boldsymbol{\lambda}/(v^{[th]} \cdot \|\boldsymbol{\lambda}\|_2)}$ ▷ Scaling
   ▷ (2) Calculating similarities $\rho_{a(i)}^{[r]}$
6:    **for all** $\hat{x}_i = \left[(t_{(i,p)}, u_{t_{(i,p)}}) \right]_{p=1}^{(nt)_i} \in C_j^{[r]}$ **do**
7:      $\rho_{a(i)}^{[r]} \leftarrow \sum_{p=1}^{(nt)_i} u_{t_{(i,p)}} \cdot \lambda_{t_{(i,p)}}$
   ▷ (3) Constructing mean-inverted indexes
8:    **for all** term ID s of $\lambda_s > 0$ **do**   ▷ Initialize $q \leftarrow 1$
9:      $(c_{(s,q)}, v_{c_{(s,q)}}) \in \check{\xi}_s^{[r]} \subset \check{\mathcal{M}}^{[r]} \leftarrow (j, \lambda_s)$ ▷ q++
10:      **if** $s \geq t^{[th]}$ and $\lambda_s < v^{[th]}$ **then**
11:        $w_{(s,j)} (\in \check{\xi}_s^{[r]} \subset \check{\mathcal{M}}^{p[r]}) \leftarrow \lambda_s$
   ▷ (4) and (5) Structuring $\check{\xi}_s^{[r]} \in \check{\mathcal{M}}^{[r]}$
12: **for all** $[\check{\xi}_s^{[r]}]_{s=1}^{t^{[th]}-1} \subset \check{\mathcal{M}}^{[r]}$ **do**
13:    Divide $[(c_{(s,q)}, v_{c_{(s,q)}})]_{q=1}^{(mf)_s}$ into two blocks of
     $[(c_{(s,q)}, v_{c_{(s,q)}})]_{q=1}^{(mfM)_s}$ and $[(c_{(s,q)}, v_{c_{(s,q)}})]_{q=(mfM)_s+1}^{(mf)_s}$.
14: **for all** $[\check{\xi}_s^{[r]}]_{s=t^{[th]}}^{D} \subset \check{\mathcal{M}}^{[r]}$ **do**
15:    Pick up tuples from $[(c_{(s,q)}, v_{c_{(s,q)}})]_{q=1}^{(mf)_s} \in \check{\xi}_s^{[r]}$ that satisfy
     $v_{c_{(s,q)}} \geq v^{[th]}$ and make $[(c_{(s,q)}, v_{c_{(s,q)}})]_{q=1}^{(mfH)_s}$ from them.
16:    Divide $[(c_{(s,q)}, v_{c_{(s,q)}})]_{q=1}^{(mfH)_s}$ into two blocks of
     $[(c_{(s,q)}, v_{c_{(s,q)}})]_{q=1}^{(mfM)_s}$ and $[(c_{(s,q)}, v_{c_{(s,q)}})]_{q=(mfM)_s+1}^{(mfH)_s}$.
   ▷ Estimating structural parameters (Sections S2 and S3)
17: **if** $r \in \{1, 2\}$ **then**
18:    $(t^{[th]}, v^{[th]}) \leftarrow$ *EstParams* $(\check{\mathcal{M}}^{[r]}, \hat{X}, \text{other arguments})$
     (detailed in Section S3)
19:    Reconstruct $\check{\mathcal{M}}^{[r]}$ using new $(t^{[th]}, v^{[th]})$

---

mean-feature values of $v_{c_{(s,q)}} \geq v^{[th]}$ are used for calculating exact partial similarities in Region 2, the tuples containing such values are placed from the top of $\check{\xi}_s^{[r]}$ to the $(mfH)_s$th entry.

(5) Structuring inverted-index arrays for the ICP filter at lines 12 to 13 in Region 1 and at line 16 in Region 2.

Furthermore, at the first and second iterations, two structural parameters $t^{[th]}$ and $v^{[th]}$ are estimated by using *EstParams* function in Sections S2 and S3. $\check{M}^{p[r]}$ is constructed after the structural-parameter estimation and then $\check{M}^{[r]}$ is updated.

S2   OBJECTIVE FUNCTION IN SECTION 5

We derive Prob $(\rho^{[ub]}(i) \geq \rho_{a(i)}; s', h)$ in Eq. (10) where s' denotes a candidate of $t^{[th]}$ and h represents $v_h^{[th]}$ that is the hth candidate of $v^{[th]}$ and the objective function in Eq. (6) by using the following three assumptions (ASMs).

ASM 1 A distribution of similarities of the ith object to centroids that are more than or equal to an average similarity $\bar{\rho}(i)$ is expressed as the following distribution in an exponential family:

$$F(\rho|\rho \geq \bar{\rho}(i)) = b \cdot e^{-a(\rho - \bar{\rho}(i))}, \tag{S1}$$

where the similarity distribution ρ is considered with a coutinuous relaxation of the descrete values ρ_j that denotes the similarity of x_i to the jth centroid, and a and b are parameters.

ASM 2 The distribution of ρ is one of the exponential family and the definite integral value from a median of ρ to the infinity of $F(\rho)$ can be regarded as that from an average of ρ to the infinity. This leads to the following equation:

$$\int_{\bar{\rho}(i)}^{\infty} F(\rho)\, d\rho = \frac{b}{a} = \frac{1}{e}. \tag{S2}$$

ASM 3 Similarity-upper-bound distribution $F^{[ub]}(\rho)$ is expressed by the parallel translation of $F(\rho)$ by $\Delta\bar{\rho}(i; s', h)$ as

$$F^{[ub]}(\rho - \Delta\bar{\rho}(i; s', h)) = F(\rho) \tag{S3}$$
$$\Delta\bar{\rho}(i; s', h) = \bar{\rho}^{[ub]}(i; s', h) - \bar{\rho}(i),$$

where the second equation is the same as Eq. (11).

Since an object belongs to a distinct cluster, i.e., hard clustering, the following equation holds:

$$\int_{\rho_{a(i)}}^{\infty} F(\rho)\, d\rho = \left(\frac{1}{e}\right) e^{-a(\rho_{a(i)} - \bar{\rho}(i))} = \frac{1}{K}, \tag{S4}$$

where $\rho_{a(i)}$ denotes the similarity of the ith object to the centroid of the cluster which the object belongs to. For simplicity, the superscript of $[r]$ for $\rho_{a(i)}^{[r]}$, which represents the rth iteration, is omitted. For the first equality in Eq. (S4), Eq. (S2) is used. Using Eqs. (S2) and (S4), the parameters a and b in Eq. (S1) are expressed as

$$a = \frac{\log(K/e)}{\rho_{a(i)} - \bar{\rho}(i)} \quad \text{and} \quad b = \frac{a}{e}. \tag{S5}$$

Then, the probability in Eq. (9) is expressed by

$$\text{Prob}\,(\rho^{[ub]}(i) \geq \rho_{a(i)}; s', h) \tag{S6}$$
$$= \int_{\rho_{a(i)} - \Delta\bar{\rho}(i; s', h)}^{\infty} F(\rho)\, d\rho = \left(\frac{1}{K}\right)\left(\frac{K}{e}\right)^{\frac{\Delta\bar{\rho}(i; s', h)}{\rho_{a(i)} - \bar{\rho}(i)}}.$$

Eq. (9) is rewritten as

$$(\check{\varphi}3)_{(s', h)} = \sum_{i=1}^{N} (ntH)_{(i; s')} \cdot \left(\frac{K}{e}\right)^{\frac{\Delta\bar{\rho}(i; s', h)}{\rho_{a(i)} - \bar{\rho}(i)}}.$$

$\Delta\bar{\rho}(i; s', h)$ is obtained by substituting $\bar{\rho}(i)$ and $\bar{\rho}^{[ub]}(i; s', h)$ in Eqs. (S7) and (S8) into Eq. (S3).

$$\bar{\rho}(i) = \sum_{p=1}^{(nt)_i} \left(u_{t_{(i,p)}} \cdot \frac{1}{K} \sum_{q=1}^{(mf)_s} v_{c_{(s,q)}} \right) \quad \text{and} \quad s = t_{(i,p)}, \quad \text{(S7)}$$

where $t_{(i,p)}$ and $c_{(s,q)}$ denote the term ID appeared at the pth position in $\hat{x}_i$ and the mean ID (cluster ID) appeared at the qth position in the inverted-index-array with the sth term ID (see Table 1).

$$\bar{\rho}^{[ub]}(i; s', h) = \sum_{s=1}^{s'-1} \left(u_s \cdot \frac{1}{K} \sum_{q=1}^{(mf)_s} v_{c_{(s,q)}} \right)$$
$$+ \sum_{s=s'}^{D} u_s \cdot \frac{1}{K} \left\{ \sum_{q=1}^{(mfH)_s} v_{c_{(s,q)}} + v_h^{[th]}((mf)_s - (mfH)_s) \right\}, \quad \text{(S8)}$$

where $(mfH)_{(s,v_h^{[th]})}$ is simplified as $(mfH)_s$ and u_s is $u_{t_{(i,p)}}$ if $u_{t_{(i,p)}}$ exits for $t_{(i,p)} \geq t^{[th]}$, 0 otherwise.

We can obtain the objective funciton by substituting Eqs. (7), (8), and (12) into Eq. (6) as

$$J(s', v_h^{[th]}) = \sum_{s=1}^{s'-1}(df)_s \cdot (mf)_s$$
$$+ \sum_{s=s'}^{D}(df)_s \cdot (mfH)_{(s,v_h^{[th]})} + \sum_{i=1}^{N}(ntH)_{(i,s')} \cdot \left(\frac{K}{e}\right)^{\frac{\Delta\bar{\rho}(i;s',h)}{\rho_{a(i)}-\bar{\rho}_i}} .$$

S3 PARAMETER ESTIMATION IN SECTION 5

This section describes our proposed efficient practical algorithm for simultaneously estimating $t^{[th]}$ and $v^{[th]}$. For the parameter estimation, we suppose that an appropriate $t^{[th]}$ exists near D on the grounds of the universal characteristics (UCs) in Section 3, i.e., the skewed forms of both the document frequency (df) and mean frequency (mf) with respect to term ID sorted in ascending order of df in Figs. 2 and 3, and $v^{[th]}$ is in the range of small values due to the skewed form of the mean-feature-values in each inverted-index array. This allows us to narrow down a search space for the two parameters.

The estimation algorithm minimizes the objective function in Eq. (6) that is rewritten as

$$(t^{[th]}, v^{[th]}) = \underset{\substack{v_h^{[th]} \in V^{[th]} \\ s_{(min)} \leq s' \leq D}}{\arg\min} \left(J(s', v_h^{[th]}) \right)$$

$$J(s', v_h^{[th]}) = \tilde{\phi}_{(s',h)} = (\phi 1)_{s'} + (\phi 2)_{(s',h)} + (\tilde{\phi} 3)_{(s',h)},$$

where s' denotes the term ID that is a candidate of $t^{[th]}$ and decremented one by one from D to the pre-determined minimum term ID of $s_{(min)}$ and h represents the hth candidate of $v^{[th]}$, i.e., $v_h^{[th]}$. Based on the presumption of $t^{[th]}$ exists near D, the estimation algorithm efficiently calculates $\tilde{\phi}_{(s',h)}$ for each $v_h^{[th]}$[1] by exploiting

---

[1]This process for each $v_h^{[th]}$ is executed in parallel processing.

a recurrence relation with respect to s' expressed by

$$\tilde{\phi}_{(s';h)} = \tilde{\phi}_{(s'+1;h)} - (df)_{s'} \cdot (mfL)_{(s';v_h^{[th]})}$$
$$+ (\tilde{\phi} 3)_{(s';h)} - (\tilde{\phi} 3)_{(s'+1;h)} \quad \text{(S9)}$$

$$\tilde{\phi}_{(D+1;h)} = \sum_{s=1}^{D}(df)_s \cdot (mf)_s \triangleq \phi$$

$$(\tilde{\phi} 3)_{(D+1;h)} = 0,$$

where $(mfL)_{(s';v_h^{[th]})} = (mf)_{s'} - (mfH)_{(s';v_h^{[th]})}$, i.e., $(mfL)_{(s';v_h^{[th]})}$ denotes the number of centroids whose feature values are lower than $v_h^{[th]}$.

Moreover, $(\tilde{\phi} 3)_{(s';h)}$ itself in Eq. (S9) is represented with a recurrence relation. We rewrite the approximate number of multiplications with respect to the ith object in Eq. (12) as

$$(\bar{\phi} 3)_{(i,s';h)} = (ntH)_{(i,s')} \cdot \left(\frac{K}{e}\right)^{\frac{\bar{\rho}^{[ub]}(i,s';h)-\bar{\rho}_i}{\rho_{a(i)}-\bar{\rho}_i}} . \quad \text{(S10)}$$

We consider two cases of the ith object contains the term whose ID is s', i.e., $s' \in \{t_{(i,p)}\}_{p=1}^{(nt)_i}$, and the other. In the latter case, $(\bar{\phi} 3)_{(i,s';h)}$ is invariant from $(\bar{\phi} 3)_{(i,s'+1;h)}$ as

$$(\bar{\phi} 3)_{(i,s';h)} = (\bar{\phi} 3)_{(i,s'+1;h)} . \quad \text{(S11)}$$

In the former case, we derive the recurrence relation while focusing on $(ntH)_{(i,s')}$ and $\bar{\rho}^{[ub]}(i, s'; h)$ in Eq. S10. First, the following equation with respect to $(ntH)_{(i,s')}$ holds.

$$(ntH)_{(i,s')} = (ntH)_{(i,s'+1)} + 1 . \quad \text{(S12)}$$

Next, $\bar{\rho}^{[ub]}(i, s'; h)$ is expressed by

$$\bar{\rho}^{[ub]}(i, s') = \bar{\rho}^{[ub]}(i, s'+1)$$
$$+ \underbrace{\left\{ \sum_{q=(mfH)_{s'}+1}^{(mf)_{s'}} (v_h^{[th]} - v_{c_{(s,q)}}) + (K - (mf)_{s'})v_h^{[th]} \right\} \left(\frac{u_{s'}}{K}\right)}_{\Delta\bar{v}_{(i,s')} \cdot u_{s'}} \quad \text{(S13)}$$

where $u_{s'}$ denotes $u_{t_{(i,p)}=s'}$ and $\Delta\bar{v}_{(i,s')}$ is the average difference between $v_h^{[th]}$ and the exact mean-feature values in Region 3 at the s'th term ID. Then, $\bar{\rho}^{[ub]}(i, s'; h)$ is expressed with the recurrence relation as

$$(\tilde{\phi} 3)_{(i,s';h)} = (ntH)_{(i,s')} \cdot \left(\frac{K}{e}\right)^{\frac{\bar{\rho}^{[ub]}(i,s')-\bar{\rho}_i}{\rho_{a(i)}-\bar{\rho}_i}}$$
$$= \left(\frac{K}{e}\right)^{\gamma(i,s')} \left[\{(ntH)_{(i,s'+1)}+1\} \left(\frac{K}{e}\right)^{\frac{\bar{\rho}^{[ub]}(i,s'+1)-\bar{\rho}_i}{\rho_{a(i)}-\bar{\rho}_i}} \right] \quad \text{(S14)}$$

$$\gamma(i, s') = \frac{\Delta\bar{v}_{(i,s')} \cdot u_{s'}}{\rho_{a(i)} - \bar{\rho}_i}, \quad \text{(S15)}$$

where the values in the square bracket are already obtained at the $(s'+1)$th term ID. The boundary conditions are set as

$$(\tilde{\phi} 3)_{(i,D+1;h)} = 0, \quad (ntH)_{(i,D+1)} = 0, \quad \bar{\rho}^{[ub]}(i, D+1) = \bar{\rho}_i . \quad \text{(S16)}$$

By applying Eqs. (S11) and (S14) to Eq. (S9), we make the recurrence relation. To efficiently calculate $\tilde{\phi}_{(s';h)}$ with it, we structure the data-object set.

Algorithm S4 Parameter-estimation function: *EstParams*

Input: $\check{\mathcal{M}}, \hat{\mathcal{X}}, \check{\mathcal{X}}^p, V^{[th]} = \left\{v_1^{[th]}, \cdots, v_{|V^{[th]}|}^{[th]}\right\}, s_{(min)}$

Output: $\left(t^{[th]}, v^{[th]}\right)$

    ▷ Initialization
1: $\phi = \sum_{s=1}^{D}(df)_s \cdot (mf)_s$
2: **for all** $\hat{x}_i \in \hat{\mathcal{X}}$ **do**
3:      $\bar{\rho}_i \leftarrow (1/K) \sum_{p=1}^{(ntH)_i} \sum_{q=1}^{(mf)^{s=t_{(i,p)}}} (v_{c_{(s,q)}} \cdot u_{t_{(i,p)}})$
    ▷ Parallel processing
4: **for all** $v_h^{[th]} \in V^{[th]}$ **do**
5:      $\tilde{\phi}_{(D+1,h)} \leftarrow \phi$
6:      $(ntH)_{(i,D+1)} \leftarrow 0, \ \Delta v_{(i,D+1)} \leftarrow 0 \quad \text{for} \ \ 1 \leq i \leq N$
7:      **for** $s' \leftarrow D$ **to** $s_{(min)}$ **do**   ▷ $s': t^{[th]}$ candidate
8:          **for all** $i = o_{(s',q)} \in \check{\eta}_{s'} \subset \check{\mathcal{X}}^p$ **do**
9:              $\tilde{\phi}_{(s',h)} \leftarrow \tilde{\phi}_{(s'+1,h)} - (ntH)_{(i,s'+1)}(K/e)^{\gamma_{(i,s'+1)}}$
10:             $\Delta v_{(i,s')} \leftarrow \Delta v_{(i,s'+1)} + \sum_{q=(mfH)'_s+1}^{(mf)_{s'}} (v_h^{[th]} - v_{c_{(s',q)}})$
                               $+ (K - (mf)_{s'}) \cdot v_h^{[th]}$
11:             $\Delta \bar{v}_{(i,s')} \leftarrow \Delta v_{(i,s')}/K$
12:             $\gamma_{(i,s')} \leftarrow (\Delta \bar{v}_{(i,s')} \cdot \check{u}_i)/(\rho_{a(i)} - \bar{\rho}_i)$
13:             $\tilde{\phi}_{(s',h)} \leftarrow \tilde{\phi}_{(s',h)} + (ntH)_{(i,s')}(K/e)^{\gamma_{(i,s')}}$
14:          $\tilde{\phi}_{(s',h)} \leftarrow \tilde{\phi}_{(s',h)} - (df)_{s'} \cdot (mfL)_{(s';v_h^{[th]})}$
15:          $J(s', v_h^{[th]}) = \tilde{\phi}_{(s',h)}$
16:      $(t_h^{[th]}, v_h^{[th]}) \leftarrow \arg\min_{s_{(min)} \leq s' \leq D} \left(J(s', v_h^{[th]})\right)$
17: $(t^{[th]}, v^{[th]}) \leftarrow \arg\min_{1 \leq h \leq |V^{[th]}|} \left(J(t_h^{[th]}, v_h^{[th]})\right)$

Table S1: Notation for *EstParams* function

Symbol	Description and Definitions
$J(s', v_h^{[th]})$	**Function** of $(s', v_h^{[th]})$ that returns the approximation number of the multiplications s': Term ID as $t^{[th]}$ candidate $v_h^{[th]}$: Mean-feature-value as $v^{[th]}$ candidate $v_h^{[th]}$ can be represented with h for simplicty.
$V^{[th]}$	**Set** of $v^{[th]}$ candidates, $v_h^{[th]}$, $h = 1, \cdots, |V^{[th]}|$
$(\tilde{\phi})_{(s',h)}$	Approximate number of multiplications for similarity calculations, given s' and h
$(df)_s$	Document frequency of sth term ID
$(mf)_s$	Mean frequency of sth term ID
$s_{(min)}$	Minimum term ID of candidates (s') of $t^{[th]}$, $s_{(min)} \leq s' \leq D$
$\check{\mathcal{X}}^p$	**Partial inverted-index** of objects, each column of which is object-tuple array $\check{\eta}_s$, $s \geq s_{(min)}$ $\check{\eta}_s = [(o_{(s,q')}, \check{u}_{o_{(s,q')}})]_{q'=1}^{(df)_s}$ $o_{(s,q')}$: q'th object ID appeared in $\check{\eta}_s$ $\check{u}_{o_{(s,q')}}$: q'th feature value appeared in $\check{\eta}_s$ $(df)_s$: Document frequency of term ID, s
$\bar{\rho}_i$	Average similarity of ith object to all centroids
$(ntH)_{(i,t^{th})}$	Number of terms in ith object whose ID is higher than or equal to given $t^{[th]}$
$(mfH)_{(s;v_h^{[th]})}$	Mean frequency of term ID s where $v_{(s,q)} \geq v_h^{[th]}$, where q is a position in $\check{\xi}_s$, given $v_h^{[th]}$
$(mfL)_{(s;v_h^{[th]})}$	$(mfL)_{(s;v_h^{[th]})} = (mf)_s - (mfH)_{(s;v_h^{[th]})}$

When using the recurrence relation, we need to access a data-object- and a mean-feature value at the sth term ID. Although the mean-feature value is accessed with the mean-inverted index $\check{\mathcal{M}}$, it is difficult to select only the data-object feature value with the current data structure of $\hat{\mathcal{X}}$ with a low computational cost. To overcome the difficulty in the architecture-friendly manner (AFM) in Section 2, we introduce a partial object-inverted-index $\check{\mathcal{X}}^p$ for the term IDs from $s_{(min)}$ to D with low memory consumption. By using the partial object-inverted-index, we can access both the feature values at the sth term ID without using conditional branches causing many mispredictions or loading the large array of the object data set, resulting in calculating $(\tilde{\phi}3)_{(i,s';h)}$ efficiently.

Algorithm S4 and Table S1 show a pseudocode of the practical algorithm *EstParams* and its notation, respectively. Given the $v^{[th]}$ candidate $v_h^{[th]} \in V^{[th]}$, at lines 4 to 16, the tuple of $(t_h^{[th]}, v_h^{[th]})$ is obtained for each $v_h^{[th]}$, where $t_h^{[th]}$ denotes the s' that minimizes $J(s', v_h^{[th]})$. At line 17, $(t^{[th]}, v^{[th]})$ is determined as the tuple that minimizes $J(t_h^{[th]}, v_h^{[th]})$ among all the tuples. At lines 7 to 15, the recurrent relation is used with the initial state of $s' = D$. By using the inverted-index-array $\check{\eta}_{s'}$ in the data-object inverted index $\check{\mathcal{X}}^p$, we can efficiently access the object-feature value $\check{u}_i$ having the s' term ID and calculate the approximate number of the multiplications $\tilde{\phi}_{(s',h)}$ at lines 8 to 15.

To confirm the effectiveness of the parameter-estimation algorithm *EstParams* in Algorithm S4, we incorporated it to our proposed K-means clustering algorithm AF-ICP in Section 4 and applied AF-ICP with $K = 80\,000$ to the 8.2M-sized PubMed data set

in Section 6. We executed *EstParams* twice, at the first and the second iteration, in AF-ICP. The purpose of its execution at the first iteration is only to reduce the elapsed time in the second iteration. Clustering results at the first iteration strongly depends on initial settings and some centroids often change their positions significantly. At the second iteration, *EstParams* determines parameter values that are utilized at the successive iterations.

We compared the approximate number of the multiplications obtained by *EstParams* with the corresponding actual number calculated by AF-ICP, where $t^{[th]}$ and $v^{[th]}$ were set at the values estimated at the second iteration. Figure S1 shows the comparison with the approximate and actual number of the multiplications along $v_h^{[th]}$ at which $t_h^{[th]}$ at line 16 in Algorithm S4 was a different value except the small $v_h^{[th]}$ values. The parameters in *EstParams* were set as $s_{(min)} = 1.22 \times 10^5$ and $0.020 \leq v_h^{[th]} \leq 0.060$ by 0.001 step. We observed that the approximate number of the multiplications agreed with the actual number in all the range and each value of $v_h^{[th]}$. The minimum number of the multiplications was observed at the identical value of 0.038 between the estimated and the actual number. Figure S2 shows the actual number of the multiplications when $t^{[th]}$ was set at the various fixed values from 1.22×10^5 to 1.32×10^5. Comparing the approximate number of the multiplications in Fig. S1 with the actual ones in Fig. S2, we notice that the approximate number corresponds to the lowest envelop curve of the actual numbers. Thus, our parameter-estimation algorithm *EstParams* can find appropriate values for $t^{[th]}$ and $v^{[th]}$ simultaneously.
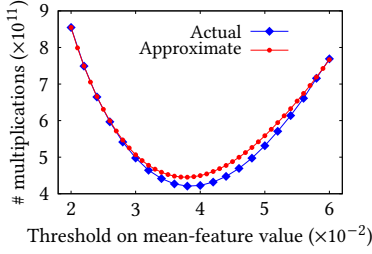
Figure S1: Comparison of the approximate and actual number of the multiplications along threshold $v_h^{[th]}$ on the mean-feature value for 8.2M-sized PubMed with K=80 000. The other threshold s' on term ID at each point differs from others in general.
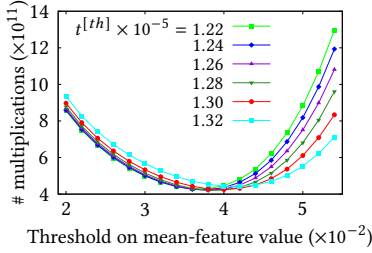
Figure S2: Actual number of the multiplications along threshold on the mean-feature value with various $t^{[th]}$ for 8.2M-sized PubMed with K=80 000.
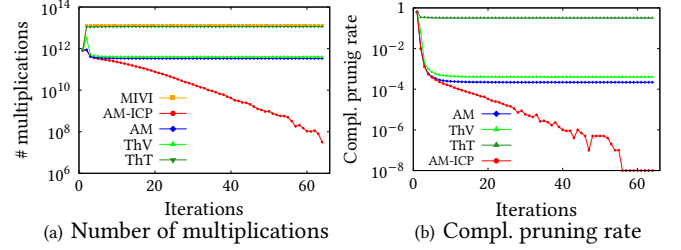
S4 ABLATION STUDY

We analyze the contributions of components in our proposed algorithm AM-ICP to its performance. We focus on the main filter AM since the performance of only the auxiliary filter ICP is evaluated in Section 6.3. The AM filter exploits the tight upper bounds on the similarities obtained by using the three regions divided by the two parameters of $t^{[th]}$ and $v^{[th]}$. We regarded the components as the two parameters and prepared three algorithms without ICP in addition to the baseline MIVI.

The first algorithm was AM that employed the two parameters. The second was ThV that utilized only the parameter $v^{[th]}$ estimated by $t^{[th]} = 0$ [2]. ThV calculated the upper-bound similarities based on the $v^{[th]}$ in the range of all the term IDs. These upper bounds were looser than AM since the exact partial similarities in Region 1 of AM were replaced with the corresponding upper bounds. For calculating the exact similarities of unpruned centroids, ThV needed mean-inverted index $\check{M}^{p[r]}$ of the memory size of $\{D \times K \times \text{sizeof(double)}\}$ bytes. The last was ThT that utilized $t^{[th]}$ estimated by $v^{[th]} = 1.0$ [3]. The upper bounds $\rho_{(j;i)}^{[ub]'}$ corresponding to those in Eq. (3) are expressed by $\rho_{(j;i)}^{[ub]'} = (\rho 1')_{(j;i)} + \|x_i^{p'}\|_1$, where $\|x_i^{p'}\|$ and $(\rho 1')_{(j;i)}$ denote the partial L_1 norm of the ith object and the exact partial similarity of the object to the jth centroid based on ThT's $t^{[th]}$.

---

[2]ThV's $v^{[th]}$ was 0.032 while AM's 0.038 for 8.2M-sized PubMed with $K = 80\,000$.
[3]ThT's $t^{[th]}$ was 140 904 while AM's 128 090 for 8.2M-sized PubMed with $K = 80\,000$.

(a) Number of multiplications (b) Compl. pruning rate

Figure S3: Ablation study in 8.2M-sized PubMed data set with K=80 000: (a) Number of multiplications and (b) Complementary pruning rate along iterations until convergence.
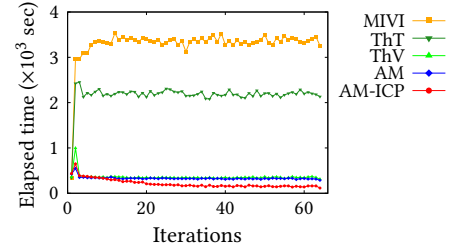
Figure S4: Elapsed time along iterations until convergence in 8.2M-sized PubMed data set with K=80 000.

Table S2: Ablation study of proposed algorithm AM-ICP in 8.2M-sized PubMed data set with K=80 000. Value in each column is rate to that of AM-ICP.

Algo.	Avg Mult	Avg time	Inst	BM	LLCM	Max MEM
AM	3.793	1.546	1.782	1.658	3.205	0.998
ThV	4.832	1.676	1.925	1.956	3.461	5.777
ThT	119.4	10.16	13.39	7.173	11.54	0.5094

Figure S3(a) and (b) show the number of the multiplications (Mult) and the complementary pruning rate (CPR) [4] along iterations until convergence when the algorithms were applied to the 8.2M-sized PubMed data set with $K = 80\,000$. AM and ThV successfully reduced both the multiplications and the CPR at the early stage in the iterations while ThT barely did. This observation shows that ThT had much looser upper bounds than AM and ThV. We know that the AM's pruning performance was mainly supported by the upper bounds based on the parameter $v^{[th]}$.

Figure S4 shows the elapsed time that each algorithm required in the same setting in Fig. S3. Table S2 shows the performance rates of the compared algorithms to AM-ICP. AM and ThV had the similar characteristics to each other in terms of the elapsed time and the performance-degradation factors of Inst, BM, and LLCM. ThV needed the high memory capacity for its partial mean-inverted index $\check{M}^{p[r]}$. We consider that the difference between these two algorithms and AM-ICP comes from the number of unpruned centroids in Fig. S3. ThT had the inferior performance to the others except the maximum memory usage. This shows that the parameter $t^{[th]}$ contributed to not the pruning performance but rather the low memory usage for the partial mean-inverted index $\check{M}^{p[r]}$ of $\{(D - t^{[th]} + 1) \times K \times \text{sizeof(double)}\}$-byte capacity. Compared with

---

[4]The values of CPR are bounded below by 1×10^{-8}.

MIVI in Table 4, ThT slightly decreased Mult and Inst with the aid of its filter while it increased BM and LLCM. This was caused by ThT's poor filter passing many centroids in Fig. S3(b). Then, many branch-mispredictions occurred in the conditional branch at the gathering phase, which judges whether $\rho_{(j;i)}^{[ub]}$ is larger than $\rho_{(max)}$ or not and mean-feature values in the partial mean-inverted index for the exact similarity calculations. were loaded many times.

The parameters of $v^{[th]}$ and $t^{[th]}$ mainly contribute to the high pruning performance and the low memory usage, respectively. The proposed algorithm AM-ICP with the two filters of AM and ICP efficiently worked at high speed and with low memory consumption from the early to the last stage in the iterations. The actual performance of AM-ICP, AM, ThV, and ThT in ablation study when they were applied to the 8.2M-sized PubMed data set with $K = 80\,000$ in Tables S3 and S4. and the 1M-sized NYT data set with $K = 10\,000$ in Tables S5 and S6.

S5 ALGORITHM PERFORMANCE IN SECTION 2

The algorithm performance of MIVI, DIVI and Ding[+] in Section 2 are shown as the rates to the baseline algorithm MIVI. This section shows the actual values in Tables S7 and S8.

S6 COMPARED ALGORITHMS IN SECTION 6.3

TA-ICP and CS-ICP in Section 6.3 are detailed. Both the algorithms employ the mean-inverted index that is partitioned by the structural parameter (threshold on term IDs) into two regions like the proposed algorithm AM-ICP. The differences from AM-ICP are in their main UBP filters and data structures related to the filters.

S6.1 TA-ICP

TA-ICP is characterized by using (1) the UBP filter every an individual object and (2) two mean-inverted indexes for moving centroids and all the centroids. Each array of the mean-inverted index is sorted in descending order of the mean-feature values. Remind that AM-ICP's array is not sorted but classified in Section 4.1. The UBP filter of TA-ICP is designed, inspired by the threshold algorithm (TA) in Fagin[+] and Li^{+} algorithms. The UBP filter utilizes a threshold ($v_{(ta)i}^{[th]}$) on mean-feature values, which is defined every the ith object as

$$v_{(ta)i}^{[th]} = \rho_{(max)} / \|x_i\|_1, \tag{S17}$$

where $\|x_i\|_1$ and $\rho_{(max)}$ denote the L_1-norm of the ith object-feature vector and the similarity of ith object to the centroid to which the object belongs at the last iteration. Due to the threshold for the individual object, it is difficult to structure the mean-inverted index when incorporating the auxiliary ICP filter unlike AM-ICP. TA-ICP employs the two mean-inverted indexes for moving and all the centroids.

Algorithms S5 and S6 show the pseudocodes of the assignment step in TA-ICP. At line 6 in Algorithm S5, the individual threshold is set. In the gathering phase from lines 7 to 11, the candidate-centroid-ID set $\mathcal{Z}_i$ for exact similarity calculations is made by the

---

Algorithm S5 Assignment step at the rth iteration in TA-ICP

1: **Input:** $\hat{\mathcal{X}}$, $\check{\mathcal{M}}^{[r-1]}$, $\check{\mathcal{M}}^{p[r-1]}$, $\left\{\rho_{a(i)}^{[r-1]}\right\}_{i=1}^N$, $t^{[th]}$,
　　　$\check{\mathcal{M}}_{mv}^{[r-1]}$

2: **Output:** $C^{[r]} = \left\{C_j^{[r]}\right\}_{j=1}^K$

3: $C_j^{[r]} \leftarrow \emptyset$, $j = 1, 2, \cdots, K$

4: **for all** $\hat{x}_i = [(t_{(i,p)}, u_{t_{(i,p)}})]_{p=1}^{(nt)i} \in \hat{\mathcal{X}}$ **do**

5: 　　$\mathcal{Z}_i \leftarrow \emptyset$, $\{\rho_j\}_{j=1}^K \leftarrow 0$, $\rho_{(max)} \leftarrow \rho_{a(i)}^{[r-1]}$,
　　　$\left\{y_{(i,j)}\right\}_{j=1}^K \leftarrow \sum_{t_{(i,p)} \geq t^{[th]}} u_{t_{(i,p)}}$

6: 　　$\boxed{v_{(ta)i}^{[th]} \leftarrow \rho_{(max)} / \|x_i\|_1}$ 　　　▷ Individual threshold

7: 　　**if** $xState = 1$ **then** 　　▷ Object satisties Eq. (4).

8: 　　　args $\leftarrow \mathcal{Z}_i$, $\{\rho_j, y_{(i,j)}\}_{j=1}^K$, $\rho_{(max)}$, $v_{(ta)i}^{[th]}$

9: 　　　$\left(\mathcal{Z}_i, \{\rho_j\}_{j=1}^K\right) = G_{(ta)1}(\text{args})$

10: 　　**else**

11: 　　　$\left(\mathcal{Z}_i, \{\rho_j\}_{j=1}^K\right) = G_{(ta)0}(\text{args})$

　　　▷ Exact-similarity calculation for unpruned centroids

12: 　　**for** $(s \leftarrow t_{(i,p)}) \geq t^{[th]}$ **do**

13: 　　　**for all** $j \in \mathcal{Z}_i$ **do**

14: 　　　　**if** $\boxed{w'_{(s,j)} < v_{(ta)i}^{[th]}}$ **then**

15: 　　　　　$\rho_j \leftarrow \rho_j + u_s \cdot w'_{(s,j)}$

　　　▷ Verification phase is the same as that in Algorithm S1.

16: 　　$C_{a(i)}^{[r]} \leftarrow C_{a(i)}^{[r]} \cup \{\hat{x}_i\}$

UBP and ICP filters. The exact similarity calculations for the centroids with IDs in $\mathcal{Z}_i$ are performed at lines 12 to 15. $w'_{(s,j)}$ at line 14 denotes the mean-feature value of the jth centroid in the sth array in the partial mean-inverted index that includes all the mean-feature values different from the AM-ICP's counter part.

Algorithm S6 Candidate-gathering function: $G_{(ta)0}$

　Input: $\hat{x}_i$, $\check{\mathcal{M}}^{[r-1]}$, $t^{[th]}$,
　　　$\mathcal{Z}_i$, $\{\rho_j, y_{(i,j)}\}_{j=1}^K$, $\rho_{(max)}$, $v_{(ta)i}^{[th]}$

　Output: $\mathcal{Z}_i$, $\{\rho_j\}_{j=1}^K$

　　▷ Exact partial similarity calculation

1: **for** $(s \leftarrow t_{(i,p)}) < t^{[th]}$ for p in $\hat{x}_i$ **do** 　　▷ Region 1

2: 　　**for** $1 \leq q \leq (mf)_s$ **do**

3: 　　　$\rho_{c_{(s,q)}} \leftarrow \rho_{c_{(s,q)}} + u_s \cdot v_{c_{(s,q)}}$

4: **for** $(s \leftarrow t_{(i,p)}) \geq t^{[th]}$ for p in $\hat{x}_i$ **do** 　　▷ Region 2-TA

5: 　　**for** $1 \leq q \leq (mf)_s$ **do**

6: 　　　$\boxed{\text{If } v_{c_{(s,q)}} < v_{(ta)i}^{[th]} \text{ then break}}$

7: 　　　$\rho_{c_{(s,q)}} \leftarrow \rho_{c_{(s,q)}} + u_s \cdot v_{c_{(s,q)}}$

8: 　　　$y_{(i,c_{(s,q)})} \leftarrow y_{(i,c_{(s,q)})} - u_s$

　　▷ Gathering phase

9: **for** $1 \leq j \leq K$ **do**

10: 　$\boxed{\text{If } \rho_j = 0 \text{ then continue}}$

11: 　$\rho_j^{[ub]} \leftarrow \rho_j + v_{(ta)i}^{[th]} \cdot y_{(i,j)}$ 　　▷ UB calculation

12: 　**if** $\rho_j^{[ub]} > \rho_{(max)}$ **then** 　　▷ UBP filter

13: 　　$\mathcal{Z}_i \leftarrow \mathcal{Z}_i \cup \{j\}$

Table S3: Ablation study in terms of average number of multiplications and average elapsed time until convergence in 8.2M-sized PubMed data set with K=80 000. Number of iterations until convergence is 64.

Algorithm	Avg. # multiplications per iteration	Avg. elapsed time per iteration (sec): [assignment, update][†]	Maximum memory size (GB)
AM-ICP	9.391×10^{10}	2.138×10^2 [185.5, 28.79]	16.72
AM	3.562×10^{11}	3.306×10^2 [304.0, 27.00]	16.69
ThV	4.538×10^{11}	3.584×10^2 [329.37, 29.50]	96.59
ThT	1.122×10^{13}	2.172×10^3 [2148.9, 23.81]	8.52

[†] The average elapsed time does not match the sum of the assignment and the update time because the algorithm terminated at the end of the assignment step of the last iteration.

Table S4: Ablation study in terms of perf results until convergence in 8.2M-sized PubMed data set with K=80 000. Number of iterations until convergence is 64.

Algorithm	# instructions	# branches	# branch misses (%)	# LLC-loads	# LLC-loads misses (%)
AM-ICP	6.157×10^{14}	8.417×10^{13}	9.569×10^{10} (0.11)	1.043×10^{13}	1.738×10^{12} (16.7)
AM	1.097×10^{15}	1.659×10^{14}	1.586×10^{11} (0.10)	3.586×10^{13}	5.569×10^{12} (15.53)
ThV	1.185×10^{15}	1.725×10^{14}	1.872×10^{11} (0.11)	4.218×10^{13}	6.015×10^{12} (14.26)
ThT	8.244×10^{15}	9.009×10^{14}	6.864×10^{12} (0.08)	2.713×10^{14}	2.004×10^{13} (7.39)

Table S5: Ablation study in terms of average number of multiplications and average elapsed time until convergence in 1M-sized NYT data set with K=10 000. Number of iterations until convergence is 81.

Algorithm	Avg. # multiplications per iteration	Avg. elapsed time per iteration (sec): [assignment, update][†]	Maximum memory size (GB)
AM-ICP	2.411×10^{10}	15.77 [5.394, 10.50]	7.914
AM	9.411×10^{10}	26.00 [15.72, 10.41]	7.907
ThV	1.430×10^{11}	32.79 [21.99, 10.94]	43.00
ThT	2.385×10^{12}	238.5 [229.6, 9.016]	4.752

[†] The average elapsed time does not match the sum of the assignment and the update time because the algorithm terminated at the end of the assignment step of the last iteration.

Table S6: Ablation study in terms of perf results until convergence in 1M-sized NYT data set with K=10 000. Number of iterations until convergence is 81.

Algorithm	# instructions	# branches	# branch misses (%)	# LLC-loads	# LLC-loads misses (%)
AM-ICP	7.003×10^{13}	1.239×10^{13}	4.127×10^{10} (0.33)	8.470×10^{11}	1.044×10^{11} (12.3)
AM	1.538×10^{14}	1.993×10^{13}	7.044×10^{10} (0.35)	3.046×10^{12}	2.727×10^{11} (8.95)
ThV	1.931×10^{14}	2.324×10^{13}	7.395×10^{10} (0.32)	3.408×10^{12}	4.071×10^{11} (11.95)
ThT	2.017×10^{15}	2.091×10^{14}	8.155×10^{10} (0.04)	2.508×10^{13}	2.215×10^{12} (8.83)

Algorithm S6 shows the pseudocode of the candidate-gathering function $G_{(ta)0}$ at line 11 in Algorithm S5. $G_{(ta)0}$ is used for the object that does not satisfy the condition in Eq. (4). When calculating the exact partial similarity of the ith object to the centroids whose ID is $c_{(s,q)}$, $G_{(ta)0}$ judges whether its feature value satisfies the condition of $v_{c_{(s,q)}} \geq v_{(ta)i}^{[th]}$ or not at line 6. After the exact partial-similarity calculations in Regions 1 and 2-TA, the upper bound on the similarity to the centroid whose exact partial-similarity is not zero is calculated. If the exact partial-similarity is zero, the upper bound is smaller than or equal to $\rho_{(max)}$ from the definition of $v_{(ta)i}^{[th]} = \rho_{(max)} / \|x_i\|_1$. In the gathering phase, the centroid-IDs of the centroids passing through the TA filter are collected in $\mathcal{Z}_i$.

Table S7: Performance of MIVI, DIVI, and Ding$^+$ in 8.2M-sized PubMed data set with K=80 000. Number of iterations unitl convergence is 64.

Algorithm	Avg. # multiplications per iteration	Avg. elapsed time per iteration (sec)
MIVI	1.326×10^{13}	3.294×10^3
DIVI	1.326×10^{13}	3.372×10^4
Ding$^+$	3.029×10^{12}	9.552×10^3

Table S8: perf results of MIVI, DIVI, and Ding$^+$ in 8.2M-sized PubMed data set with K=80 000. Number of iterations unitl convergence is 64.

Algorithm	# instructions	# branches	# branch misses (%)	# LLC-loads	# LLC-loads misses (%)
MIVI	1.032×10^{16}	9.704×10^{14}	3.770×10^{11} (0.04)	2.772×10^{14}	1.724×10^{13} (6.22)
DIVI	1.006×10^{16}	1.019×10^{15}	2.743×10^{12} (0.27)	7.983×10^{14}	6.444×10^{14} (80.7)
Ding$^+$	6.691×10^{15}	1.949×10^{15}	1.937×10^{14} (9.94)	6.637×10^{14}	6.577×10^{14} (99.1)

The function $G_{(ta)1}$ at line 9 in Algorithm S5 has the identical structure to $G_{(ta)0}$. The difference is that $G_{(ta)1}$ uses the moving-centroid mean-inverted index instead of $\check{\mathcal{M}}^{[r-1]}$. For this difference, $(mf)_s$ at lines 2 and 5 in $G_{(ta)0}$ is replaced with $(mfM)_s$ in $G_{(ta)1}$.

S6.2 CS-ICP

CS-ICP is characterized by using (1) the Cauchy-Schwarz inequality that is applied to mean-feature vectors in a subspace of an individual object-feature vector, (2) an additional mean-inverted index that stores squared mean-feature values, and (3) no threshold on the mean-feature values unlike AM-ICP and TA-ICP.

Algorithm S7 Assignment step at the rth iteration in CS-ICP

Input: $\hat{X}$, $\check{\mathcal{M}}^{[r-1]}$, $\check{\mathcal{M}}^{p[r-1]}$, $\left\{\rho_{a(i)}^{[r-1]}\right\}_{i=1}^{N}$, $\left\{\|x_i^p\|_2\right\}_{i=1}^{N}$, $\check{\mathcal{M}}_{sq}^{p[r-1]}$, $t^{[th]}$

Output: $C^{[r]} = \left\{C_j^{[r]}\right\}_{j=1}^{K}$

1: $C_j^{[r]} \leftarrow \emptyset$, $j = 1, 2, \cdots, K$
2: **for all** $\hat{x}_i = [(t_{(i,p)}, u_{t_{(i,p)}})]_{p=1}^{(nt)_i} \in \hat{X}$ **do**
3: $\quad \{\rho_j\}_{j=1}^{K} \leftarrow 0$, $\mathcal{Z}_i \leftarrow \emptyset$, $\rho_{(max)} \leftarrow \rho_{a(i)}^{[r-1]}$
4: $\quad$ **if** $xState = 1$ **then** $\triangleright$ Object satisties Eq. (4).
5: $\qquad \left(\mathcal{Z}_i, \{\rho_j\}_{j=1}^{K}\right) = G_{(cs)1}(\mathcal{Z}_i, \{\rho_j\}_{j=1}^{K}, \rho_{(max)})$
6: $\quad$ **else**
7: $\qquad \left(\mathcal{Z}_i, \{\rho_j\}_{j=1}^{K}\right) = G_{(cs)0}(\mathcal{Z}_i, \{\rho_j\}_{j=1}^{K}, \rho_{(max)})$

$\quad\triangleright$ Exact-similarity calculation for unpruned centroids
$\quad\triangleright$ Verification phase
$\quad\triangleright$ These two parts are the same as those in Algorithm S1.
8: $\quad C_{a(i)}^{[r]} \leftarrow C_{a(i)}^{[r]} \cup \{\hat{x}_i\}$

Algorithm S7 shows the pseudocode of the assignment step in CS-ICP. $\|x_i^p\|_2$ and $\check{\mathcal{M}}_{sq}^{p[r-1]}$ in the inputs denote the L_2-norm of the ith object's *partial* feature vector and the *partial* squared mean-inverted index in the range of $t_{(i,p)} \geq t^{[th]}$, respectively. At

lines 5 to 7, the candidate centroids for the exact similarity calculations are collected by the candidate-gathering functions $G_{(cs)0}$ and $G_{(cs)1}$. The other parts are the same as those in Algorithm S1.

Algorithm S8 Candidate-gathering function: $G_{(cs)0}$

Input: $\hat{x}_i$, $\check{\mathcal{M}}^{[r-1]}$, $\mathcal{Z}_i$, $\{\rho_j\}_{j=1}^{K}$, $\rho_{(max)}$, $t^{[th]}$, $\|x_i^p\|_2$, $\check{\mathcal{M}}_{sq}^{p[r-1]}$

Output: $\mathcal{Z}_i$, $\{\rho_j\}_{j=1}^{K}$

1: $\{\|\mu_j^p\|_2^2\}_{j=1}^{K} \leftarrow 0$ $\triangleright$ Initialization
$\quad\triangleright$ Exact partial similarity calculation
2: **for** $(s \leftarrow t_{(i,p)}) < t^{[th]}$ in all term IDs in $\hat{x}_i$ **do**
3: $\quad$ **for** $1 \leq q \leq (mf)_s$ **do**
4: $\qquad \rho_{c_{(s,q)}} \leftarrow \rho_{c_{(s,q)}} + u_s \cdot v_{c_{(s,q)}}$
$\quad\triangleright$ Calculate squared mean-L2-norm in object-subspace
5: **for** $(s \leftarrow t_{(i,p)}) \geq t^{[th]}$ in all term IDs in $\hat{x}_i$ **do**
6: $\quad$ **for** $1 \leq q \leq (mf)_s$ **do**
7: $\qquad \boxed{\|\mu_{c_{(s,q)}}^p\|_2^2 \leftarrow \|\mu_{c_{(s,q)}}^p\|_2^2 + v_{c_{(s,q)}}^2}$
$\quad\triangleright$ Gathering phase
8: **for** $1 \leq j' \leq (nMv)$ **do** $\triangleright$ nMv: #moving centroids
9: $\quad j'$ is transformed to j.
10: $\quad \boxed{\rho_j^{[ub]} \leftarrow \rho_j + \|x_i^p\|_2 \times \sqrt{\|\mu_j^p\|_2^2}}$ $\triangleright$ UB calculation
11: $\quad$ **if** $\rho_j^{[ub]} > \rho_{(max)}$ **then** $\triangleright$ UBP filter
12: $\qquad \mathcal{Z}_i \leftarrow \mathcal{Z}_i \cup \{j\}$

Algorithm S8 shows the pseudocode of the candidate-gathering function $G_{(cs)0}$ at line 7 in Algorithm S7. $G_{(cs)0}$ is used for the object that does not satisfy the condition in Eq. (4). At lines 2 to 4, the exact partial similarities $\rho_{c_{(s,q)}}$ are calculated in the range of $t_{(i,p)} < t^{[th]}$. At lines 5 to 7, the squared L_2-norm of the partial mean-feature vector $\|\mu_{c_{(s,q)}}^p\|_2^2$ is calculated in the subspace of the ith object-feature vector, where $v_{c_{(s,q)}}^2$ denotes the squared mean-feature value in $\check{\mathcal{M}}_{sq}^{p[r-1]}$. At lines 8 to 12, the gathering phase is performed and the centroid-ID set $\mathcal{Z}_i$ for exact similarity calculations is returned. At line 10, the upper bound on the

similarity to the jth centroid $\rho_j^{[ub]}$ is calculated by the sum of the foregoing exact partial similarity ρ_j and the product of the pre-calculated L_2-norm of the ith object's partial feature vector $\|\pmb{x}_i^p\|_2$ and $\sqrt{\|\pmb{\mu}_{c_{(s,q)}}^p\|_2^2}$. In this product calculation, the square-root operation is performed, which requires high computational cost.

The function $G_{(cs)1}$ at line 5 in Algorithm S7 is similar to $G_{(cs)0}$. The difference is in the endpoint of the loops at lines 3 and 6. $G_{(cs)0}$ uses $(mf)_s$ while $G_{(cs)1}$ does $(mfM)_s$ in the mean-inverted index consisting of the moving centroids.

S6.3 Performance Comparison

This section shows the actual algorithm performance of AM-ICP, ICP, CS-ICP, and TA-ICP when they were applied to the 8.2M-sized PubMed data set with $K = 80\,000$ in Tables S9 and S10 and the 1M-sized NYT data set with $K = 10\,000$ in Tables S11 and S12.

Table S9: Performance comparison of AM-ICP, ICP, CS-ICP and TA-ICP in 8.2M-sized PubMed data set with K=80 000. Number of iterations until convergence is 64.

Algorithm	Avg. # multiplications per iteration	Avg. elapsed time per iteration (sec): [assignment, update][†]	Maximum memory size (GB)
AM-ICP	9.391×10^{10}	2.138×10^2 [185.5, 28.79]	16.72
ICP	2.960×10^{12}	7.595×10^2 [729.9, 30.05]	8.285
CS-ICP	1.733×10^{11}	9.017×10^2 [875.2, 26.99]	18.31
TA-ICP	9.069×10^{11}	1.052×10^3 [1016, 36.09]	19.07

[†] The average elapsed time does not match the sum of the assignment and the update time because the algorithm terminated at the end of the assignment step of the last iteration.

Table S10: perf results of AM-ICP, ICP, CS-ICP, and TA-ICP in 8.2M-sized PubMed data set with K=80 000. Number of iterations until convergence is 64.

Algorithm	# instructions	# branches	# branch misses (%)	# LLC-loads	# LLC-loads misses (%)
AM-ICP	6.157×10^{14}	8.417×10^{13}	9.569×10^{10} (0.11)	1.043×10^{13}	1.738×10^{12} (16.7)
ICP	2.876×10^{15}	2.934×10^{14}	2.796×10^{11} (0.10)	8.277×10^{13}	4.467×10^{12} (5.40)
CS-ICP	2.346×10^{15}	2.786×10^{14}	3.127×10^{11} (0.11)	9.297×10^{13}	8.025×10^{12} (8.63)
TA-ICP	1.761×10^{15}	3.030×10^{14}	1.853×10^{12} (0.61)	4.728×10^{13}	2.236×10^{13} (47.30)

Table S11: Performance comparison of AM-ICP, ICP, CS-ICP and TA-ICP in 1M-sized NYT data set with K=10 000. Number of iterations until convergence is 81.

Algorithm	Avg. # multiplications per iteration	Avg. elapsed time per iteration (sec): [assignment, update][†]	Maximum memory size (GB)
AM-ICP	2.411×10^{10}	15.77 [5.394, 10.50]	7.914
ICP	2.898×10^{11}	107.2 [94.03, 13.31]	4.147
CS-ICP	2.137×10^{10}	86.16 [76.89, 9.380]	8.419
TA-ICP	3.947×10^{11}	68.13 [57.22, 11.05]	8.645

[†] The average elapsed time does not match the sum of the assignment and the update time because the algorithm terminated at the end of the assignment step of the last iteration.

Table S12: perf results of AM-ICP, ICP, CS-ICP, and TA-ICP in 1M-sized NYT data set with K=10 000. Number of iterations until convergence is 81.

Algorithm	# instructions	# branches	# branch misses (%)	# LLC-loads	# LLC-loads misses (%)
AM-ICP	7.003×10^{13}	1.239×10^{13}	4.127×10^{10} (0.33)	8.470×10^{11}	1.044×10^{11} (12.3)
ICP	4.065×10^{14}	4.363×10^{13}	5.652×10^{10} (0.13)	4.734×10^{12}	4.196×10^{11} (8.86)
CS-ICP	3.437×10^{14}	4.322×10^{13}	6.778×10^{10} (0.16)	5.783×10^{12}	1.456×10^{12} (25.18)
TA-ICP	4.357×10^{14}	6.151×10^{13}	4.422×10^{11} (0.72)	7.106×10^{12}	2.162×10^{12} (30.42)